High-Resolution Vibrational Spectra of Furazan
III. The A_1 Fundamentals v_3 at $\sim 1316\ \text{cm}^{-1}$ and v_4 at $\sim 1036\ \text{cm}^{-1}$ from Fourier-Transform Infrared Spectroscopy

Otto L. Stiefvater

Coleg Prifysgol Gogledd Cymru, Bangor LL57 2UW, Wales, U.K.

With prior information on vibrationally excited states from DRM microwave spectroscopy, two B-type high-resolution FT-IR bands of furazan were examined to yield the band origins $v_3^0 = 1316.2254\ \text{cm}^{-1}$ and $v_4^0 = 1036.1689\ \text{cm}^{-1}$ with an estimated absolute uncertainty of $\pm 0.0001\ \text{cm}^{-1}$. The rotational and distortion constants of both fundamental states were refined by the combination of rotational with rovibrational data in the least-squares fits of the bands.

I. Introduction

Following the study of the pure rotational spectra [1 a] of the ground state (GS) and of twelve fundamental vibration states of the five-membered ring compound furazan ($C_2H_2N_2O$) by double resonance modulation (DRM) microwave spectroscopy [1 b] in the late 1980s, the rovibrational bands of this compound were recorded under high resolution on the FT-IR spectrometer (Bruker IFS 120 HR) at the Justus-Liebig-Universität Giessen during the summer of 1990. The purpose of that work was to establish experimental information suitable for the determination of the vibrational band origins v_i^0 with the highest possible accuracy. Accordingly, efforts since then have been focused on the rovibrational analyses of the observed bands. That task was greatly facilitated through the availability of the rotational constants of the excited states from the earlier microwave study [1 a].

In two preceding papers [1 c, d] the vibrational band origins and rotational parameters, which could be refined beyond the limit set by the microwave (MW) study, were reported for the B_1-fundamentals (A-type bands) $v_{12} \sim 953\ \text{cm}^{-1}$ and $v_{11} \sim 1175\ \text{cm}^{-1}$ and for the A_1-fundamental $v_5 \sim 1005\ \text{cm}^{-1}$. In continuation of that work, which ultimately aims at the rovibrational analysis of all IR-detectable bands of furazan, the present paper reports corresponding results for the medium-strong A_1-fundamental $v_3 \sim 1316\ \text{cm}^{-1}$ and for the weak A_1-band $v_4 \sim 1036\ \text{cm}^{-1}$. In addition to

having a small intensity, the latter band is appreciably overlapped by the R-branch of the strong A_1-band v_5.

II. Experimental, Theoretical and Computational Aspects

The high-resolution IR spectra of the bands v_3 and v_4 of furazan were obtained on the Bruker IFS 120 HR interferometer. The sample cell was an external addition to the commercial instrument and was 300 cm in length. It contained the furazan vapour at a pressure of 2.5 mbar for the study of the v_3-band and at 2 mbar for the recording of the v_4-band. In both cases the sample gas was at room temperature (300 K). The interferograms were built up from 245 scans in each case, and the unapodized spectral resolution was 0.0039 cm⁻¹ for v_3 and 0.0028 cm⁻¹ for the v_4-band. After both furazan runs, the spectrometer was calibrated against precisely known [2] absorptions of N_2O. These calibrations indicated a standard error of 8×10^{-5} cm⁻¹ of the wavenumber scale of the instrument.

The analysis of the observed bands rested on the assumption that no interactions of v_3 or v_4 with other vibrational modes were taking place and that the disposition of levels within each of the excited states was therefore adequately describable by the eigenvalues of Watson's [3] A-reduced Hamiltonian in the I^r representation,

$$\hat{H}_{\text{rot.}} = \tfrac{1}{2}(B+C)\,\hat{P}^2$$
$$+ (A - \tfrac{1}{2}(B+C))\,\hat{P}_a^2 - \Delta_J\,\hat{P}^4 - \Delta_{JK}\,\hat{P}^2\,\hat{P}_a^2 - \Delta_K\,\hat{P}_a^4$$
$$+ (\tfrac{1}{2}(B-C) - 2\delta_J\,\hat{P}^2)\cdot(\hat{P}_b^2 - \hat{P}_c^2)$$
$$+ [(-\delta_K\,\hat{P}_a^2),\,(\hat{P}_b^2 - \hat{P}_c^2)]_+ ,$$

where A, B, and C are the reduced rotational constants, Δ and δ are the quartic distortion constants and $\hat{P}$ is the angular momentum operator with components $\hat{P}_{a,b,c}$ along the principal inertial axes of the molecule. The third line in this expression is the product of the bracketed operators, and the last line represents the anti-commutator [3]. Additional terms, which reflect the contributions of sextic distortion effects, have been omitted from this Hamiltonian. This has been justified previously [1 c, d] for the GS and for the modes v_{12}, v_{11}, and v_5.

The numerical part of the analyses was carried out with the computer package developed by Gambi et al. [4] on the basis of the above assumption. It comprises two parts: A 'forward' calculation (TRANSI) of the band structure from the rotational parameters of the GS and of the excited state with a given vibrational frequency difference v^0 (band origin) between them, and the reverse procedure (SMINIQ) for extracting by a least-squares (LSQ) routine the rotational parameters and the band origin from a set of identified (assigned) rovibrational transitions of an observed band.

III. Results

A) The v_3-band at ~ 1316 cm^{-1}

1. Assignment of IR transitions

Prior knowledge [1 a] of the molecular constants of the state $v_3 = 1$ and of the GS parameters [1 a, c] allowed the structure of this B-type band to be calculated with a high degree of confidence in the results. Hence, only the band origin v_3^0 remained as a relatively uncertain quantity. This allowed merely for a shift of the band structure as a whole to higher or lower wavenumbers. On the basis of the earlier, low-resolution study of Christensen et al. [5] this amounted to an uncertainty of ± 1 cm^{-1} around their $v_3^0 = 1316$ cm^{-1}. Accordingly, the high-resolution IR trace was examined in this range for the area of maximum transmittance with a nearly symmetrical absorption pattern commencing on either side. This expectation seemed to be met by a value of $v_3^0 \sim 1316.2$ cm^{-1} with the anticipated [1 c] weak 'conjugate Q-branch transitions' (as, for example, $1_{01} \leftarrow 1_{10}$ and $1_{10} \leftarrow 1_{01}$ or the pair $2_{02} \leftarrow 2_{11}$ and $2_{11} \leftarrow 2_{02}$, etc.) apparently displaced about equally to either side.

A subsequent prediction of the complete IR band up to $J' = 50$ with $v_3^0 = 1316.2$ cm^{-1}, with the excited

Table 1. Molecular constants of the vibrational ground state of furazan.

	Rotational constants (in cm^{-1} and MHZ)	Quartic distortion constants (in 10^{-7} cm^{-1})	
A	0.348 814 617 (21)[a] 10 457.1991 (6)[b]	Δ_J	0.832 70 (18)
		Δ_{JK}	$-0.276\,00$ (59)
B	0.322 944 775 (19) 9 681.6408 (6)	Δ_K	0.768 14 (60)
		δ_J	0.332 47 (6)
C	0.167 572 473 (19) 5 023.6964 (6)	δ_K	0.625 57 (27)

[a] Uncertainties are one σ-limit and given in units of the last quoted digit.
[b] Conversion factor: $c = 299\,792\,458$ m/sec.

state constants from the earlier DRM microwave work [1 a] and with the GS constants as refined previously (Table 1 and [1 c]) allowed detailed assignments of rovibrational transitions within the v_3-band to be made with relative ease. Altogether, some 800 P-branch lines and equally many R-branch lines with J'-values up to $J' = 65$ could eventually be identified in the range from 1290 cm^{-1} to 1340 cm^{-1}. Continual refinement of the band parameters finally allowed an equal number of Q-branch transitions to be picked out within some ± 10 cm^{-1} of the band origin.

2. Qualitative Description of the v_3-Band

A general description of the B-type bands of furazan, which connect the GS with excited states of C_{2v} symmetry A_1, has been given previously [1 c]. The v_3-band is shown in the centre of Fig. 1 in a compressed presentation, and small high-resolution sections of the band are arranged around the outside of that figure. Numbers, which indicate the leading value of the principal rotational quantum number $\bar{J}'$ of the upper vibration state for each group of $|\Delta J| = 1$ transitions (clusters), are inserted in these traces. – Up to $\bar{J}' = 25$ the clusters are relatively compact and therefore leave sufficient space for the observation of the generally weaker Q-branch transitions in the wavenumber gaps between them. For higher $\bar{J}'$-values the clusters progressively spread out into these gaps which they fill completely at $\bar{J}' \sim 40-45$ (bottom left and right trace in Figure 1). Eventually, for $\bar{J}' > 45$, the low-J' members of one cluster merge with the intense high-J' members at the beginning of the next group of transitions, and this makes the recognition of the structure of the band more and more difficult at high
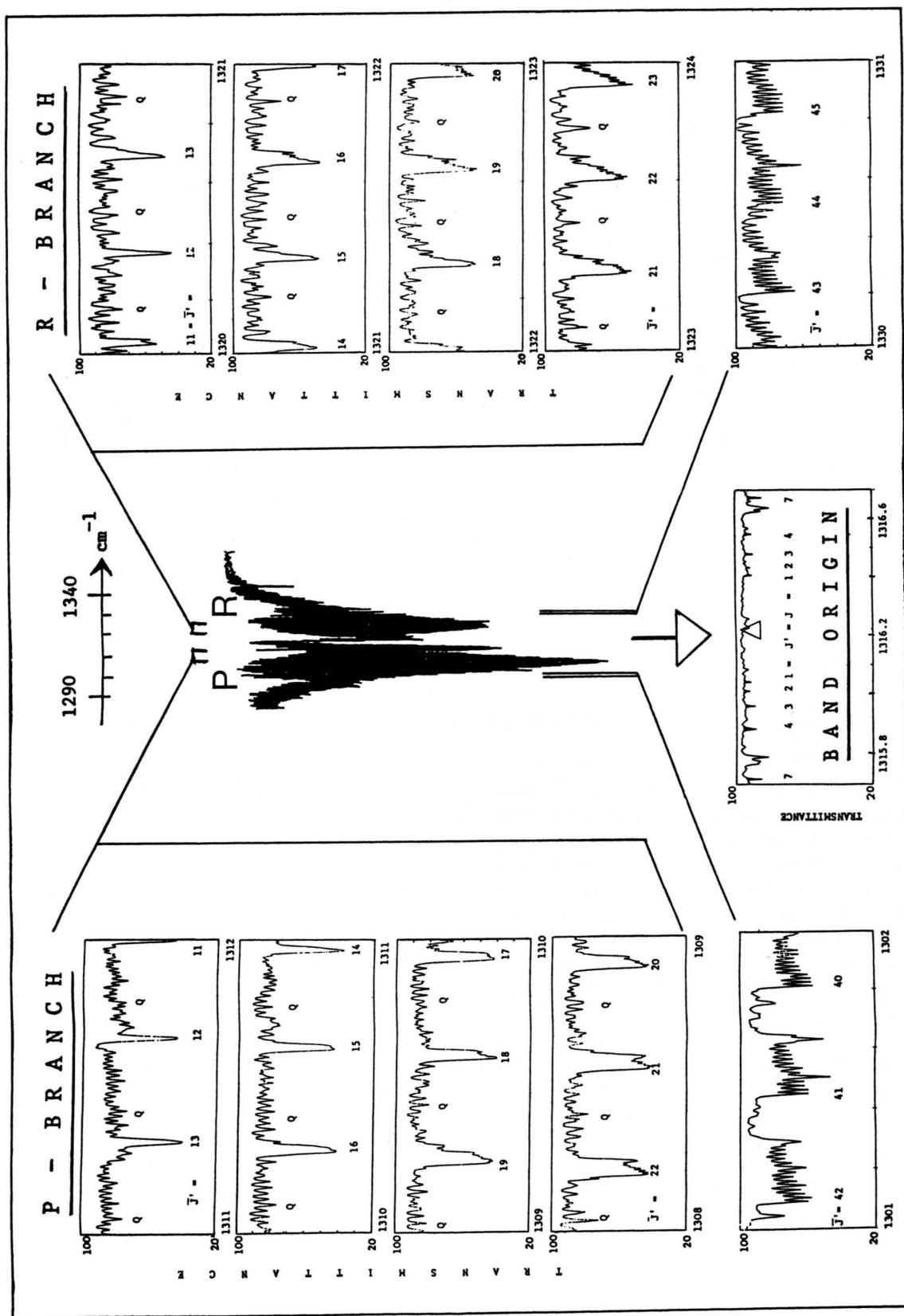
Fig. 1. The B-type band ν_3 at ~1316 cm^{-1} with high-resolution sections.

J'-values. – The Q-branch transitions of this and any other B-type band begin with the very weak 'conjugate' low-J transitions which are displaced nearly symmetrically about the band origin (middle trace, bottom of Figure 1). The identification of these pairs of 'conjugate Q-branch lines' provides a very convenient way of determining the origin of an isolated B-type band.

B) The ν_4-Band at ~ 1036 cm^{-1}

1. Assignment of IR transitions

As a consequence of the small intensity of this band and the overlap of its origin by high-J R-branch transitions ($J' > 50$) of the strong ν_5-band [1 c], the weak 'conjugate Q-branch transitions', which would indicate the band origin, could not be picked out by inspection of the trace. This entailed an uncertainty of ± 1 cm^{-1} in the probable value of the band origin $\nu_4^0 \sim 1036$ cm^{-1} [5]. However, the occurrence of successive $\Delta J = 1$ clusters in the R-branch of ν_4 was readily discernable (see Fig. 2) though the correct $\bar{J}'$-value of each cluster had to remain uncertain as a consequence of the uncertainty in ν_4^0. This insecure situation was removed by trial fits of the leading transitions of some 40 consecutive clusters together with the 89 known MW transitions within the excited state to $\bar{J}'$-values varying by $\Delta \bar{J}'$ up to ± 2 from those values which were expected on the basis that $\nu_4^0 = 1036.0$ cm^{-1} ($\Delta \bar{J}' = 0$). These trial fits were first carried out with the rotational constants of the state $\nu_4 = 1$ fixed to the values obtained from a fit of the DRM MW data alone, i.e. with only ν_4^0 variable. As the top three rows of Table 2 indicate, both the standard deviation of the fits and the uncertainty $\delta \nu_4^0$ of the resulting band origin were at least five times smaller for the assignment given in Fig. 2 ($\Delta \bar{J}' = 0$) than for the adjacent possibilities with all $\bar{J}'$-values increased or decreased by unity. As a further check on the best ν_4^0-value suggested by these calculations, a second series of trial fits was carried out, in which, in addition to ν_4^0, the rotational constants A', B', and C' were treated as adjustable. The results are given in the lower half of Table 2, and they indicate that the closest approach of A', B', and C' to the values, which were determined from the earlier DRM MW data [1a] alone, occurs for $\Delta \bar{J}' = 0$ (central column of Table 2). In summary, by far the best consistency between DRM MW and FT-IR data occurred with the $\bar{J}'$-as-

signment as indicated in Fig. 2 and resulted in $\nu_4^0 = 1036.169$ cm^{-1}. – With this value for the band origin it subsequently became possible to fit all detectable members of each cluster (about 460 R branch lines), to identify for inclusion in the fit nearly the same number of Q-branch transitions and, finally, to select some 200 assignable transitions of the overlapped P-branch of ν_4. The latter number is only half that of the assigned R-branch lines because the missing half of the P-branch lines is completely 'swamped' by the much stronger transitions of the R-branch of ν_5.

2. Qualitative Appearance of the ν_4-Band

Figure 2 shows the ν_4-band to be at least five times weaker than the neighbouring ν_5-band which has been analysed previously [1 c]. The structure of its P-branch is burried under the spread-out and much more intense R-branch clusters of ν_5, and for this reason no high-resolution sections of that part of the band are reproduced in Figure 2. Instead, the figure shows a continuous section over 14 cm^{-1} in which the emergence of the R-branch of ν_4 seems fairly obvious despite the weakness of transitions (note that the range of transmittance has been reduced from 100% in the previous papers to 50% in Figure 2). The wavenumber range reproduced under high resolution stretches from the band origin, which is not recognisable but indicated by the arrow, up to 1050 cm^{-1} and shows the fading-out of ν_5-transitions which allows the emergence of the R-branch structure of ν_4. The assigned values of $\bar{J}'$ have been inserted for each recognisable cluster.

C) Molecular Constants and Band Origins

For both bands the rotational constants and the five quartic distortion constants together with the band origin were determined from the identified rovibrational transitions together with the known MW transitions within each excited state [1 a] by the LSQ fitting procedure SMINIQ [4]. The parameters of the GS were held fixed in these fits at the values determined previously ([1 c] and Table 1).

As in the previous studies, a limit of 5×10^{-4} cm^{-1} was imposed on the acceptable differences between observed and calculated wavenumber values, and transitions with larger discrepancies were removed from the final LSQ fits. For the ν_3-band this resulted in the elimination of some 50 assignable IR transi-

Table 2. Results of the trial-fits of the leading transitions of the R-branch clusters of the weak v_4-band to different values of $\bar{J}'$ (all entries are in cm^{-1}).

$\Delta \bar{J}' =$	-2	-1	0 [a]	$+1$	$+2$
	1. Rotational constants of $v_4 = 1$ fixed to DRM MW values (only v_4^0 variable)				
St'd dev'n	0.381 E-3	0.189 E-3	0.332 E-4	0.222 E-3	0.423 E-3
v_4^0	1036.808 226	1036.488 110	1036.168 989	1035.849 866	1035.530 044
δv_4^0	. 157	. 78	. 14	. 91	. 174
	2. Rotational constants A', B', C' of $v_4 = 1$ and v_4^0 variable				
St'd dev'n	0.183 E-3	0.965 E-4	0.227 E-4	0.840 E-4	0.164 E-3
v_4^0	1036.807 730	1036.487 871	1036.169 007	1035.850 154	1035.530 551
δv_4^0	. 76	. 40	. 9	. 35	. 68
A'	0.349 231 054	0.349 214 173	0.349 197 859 [b]	0.349 182 565	0.349 168 541
$\delta A'$	. 3 494	. 1 833	. 430	. 1 554	. 3 008
B'	0.322 731 210	0.322 714 322	0.322 698 003	0.322 682 703	0.322 668 674
$\delta B'$	. 3 447	. 1 808	. 424	. 1 554	. 3 008
C'	0.167 798 407	0.167 781 306	0.167 764 790	0.167 749 313	0.167 735 127
$\delta C'$	. 1 513	. 765	. 173	. 611	. 1 141

[a] $\Delta \bar{J}' = 0$ denotes the rovibrational assignments inserted in Figure 2.
[b] The rotational constants of $v_4 = 1$, as derived from the DRM MW transitions [1 a] alone, are:
$A' = 0.349\ 201\ 144\ (494)$ cm^{-1}, $B' = 0.322\ 700\ 596\ (494)$ cm^{-1}, $C' = 0.167\ 766\ 420\ (492)$ cm^{-1}.
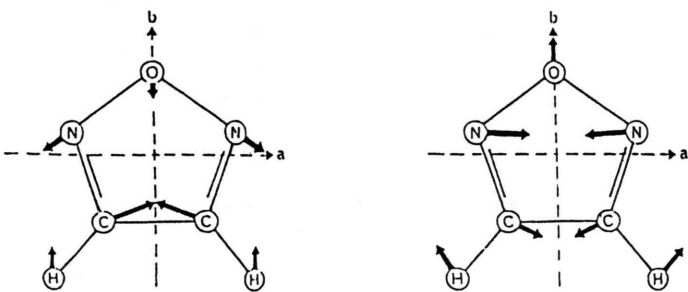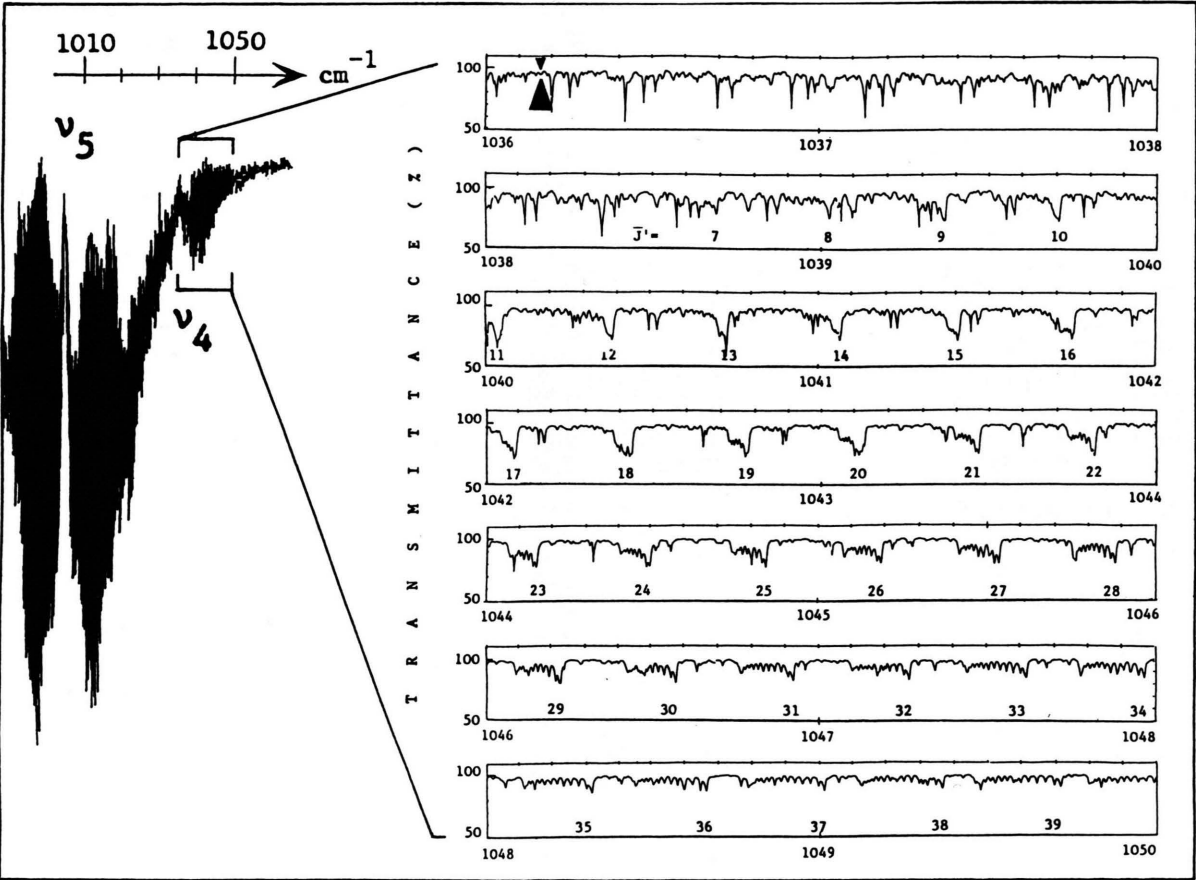

Fig. 2. The R-branch of the weak B-type band $v_4 \sim 1036$ cm^{-1} under high resolution.

tions, while in the case of the weak and partly over-lapped v_4-band some 180 rovibrational transitions had to be discarded. While the number of transitions in the LSQ fits was reduced by the imposition of the mentioned compatibility limit, an increase in this number was obtained through the splitting of ob-

served peaks into closely spaced doublets whenever the calculation indicated that an observed peak represented two experimentally unresolvable transitions. In these cases – some 150 in the v_3-band and some 50 within v_4 – half the calculated separation between the two components was added to and subtracted from

Table 3. Molecular constants and band origins for the fundamental vibrations v_3 and v_4 of furazan.

Mode, level	$v_3 = 1$	$v_4 = 1$
C_{2v} symmetry species	A_1	A_1
Selection rule/type	μ_b/B-type	μ_b/B-type
Diagrammatic Description		
Fitted transitions		
$N_{P\text{-branch}}$	833	184
$N_{Q\text{-branch}}$	811	418
$N_{R\text{-branch}}$	806	446
$N (IR)_{Total}$	2450	1048
St'd dev'n of IR fit	2.4 E-4 cm^{-1}	2.7 E-4 cm^{-1}
MW transitions	84	89
$N (IR + MW)_{Total}$	2534	1137
St'd dev'n (IR + MW)	1.3 E-5 cm^{-1}	1.0 E-5 cm^{-1}
Rotational constants (in cm^{-1} and MHz)[a]		
A	0.348 495 161 (25)[b]	0.349 200 905 (26)
	10 447.6221 (8)	*10 468.7798 (8)*
B	0.322 366 713 (23)	0.322 700 262 (24)
	9 664.3109 (7)	*9 674.3105 (7)*
C	0.167 265 480 (17)	0.167 766 710 (29)
	5 014.4929 (6)	*5 029.5194 (9)*
Quartic distortion constants (in 10^{-7} cm^{-1})		
Δ_J	0.771 19 (14)	0.845 12 (11)
Δ_{JK}	−0.141 80 (71)	−0.181 74 (72)
Δ_K	0.696 90 (92)	0.673 10 (94)
δ_J	0.304 33 (7)	0.334 91 (6)
δ_K	0.575 38 (27)	0.641 56 (29)
Band origin v^0 (in cm^{-1})	1316.225 357 (2)	1036.168 926 (2)

[a] Conversion factor $c = 299\ 792\ 458$ m/sec. – [b] Uncertainties are one σ-limit and given in units of the last quoted digit.

Correlation matrix of the LSQ determination of the molecular constants of the state $v_3 = 1$.

1.0000								
−0.0561	1.0000							
−0.2352	0.6331	1.0000						
0.3049	−0.2615	−0.6967	1.0000					
0.0674	0.1929	0.3292	−0.8251	1.0000				
0.5478	0.3212	0.3940	−0.1627	0.1970	1.0000			
−0.0246	0.4620	0.9005	−0.6197	0.2995	0.6577	1.0000		
0.2059	0.0691	0.0655	0.5441	−0.6696	0.1553	0.0224	1.0000	
0.0132	−0.1757	−0.0474	0.0043	−0.0003	0.0102	−0.0069	−0.0024	1.0000

Sequence of variables: $A - B$, B, Δ_J, Δ_{JK}, Δ_K, $B - C$, δ_J, δ_K, v_3^0.

Correlation matrix of the LSQ determination of the molecular constants of the state $v_4 = 1$.

1.0000								
−0.2835	1.0000							
−0.3500	0.6225	1.0000						
0.1788	−0.0664	−0.6524	1.0000					
0.0661	0.0723	0.4335	−0.9039	1.0000				
0.7081	−0.1849	−0.0623	−0.0433	0.1465	1.0000			
0.2966	−0.1064	0.3435	−0.4055	0.3186	0.7108	1.0000		
0.0739	−0.2038	−0.1063	0.2600	−0.4131	0.0129	−0.2290	1.0000	
0.0660	−0.1526	−0.0715	−0.0005	0.0081	0.0806	0.0563	0.0109	1.0000

Sequence of variables: $A - B$, B, Δ_J, Δ_{JK}, Δ_K, $B - C$, δ_J, δ_K, v_4^0.

the observed peak wavenumber value so as to generate two fittable values. In the listings of the fitted transitions, which have been deposited with the "Sektion für Spektren and Strukturdokumentation" of the Universität Ulm (FRG), such split wavenumber values are marked with a dot. They are easily recognisable, of course, because they show separations which are up to ten times smaller than the resolution of the spectrometer (~ 0.004 cm^{-1}).

As may be seen from Table 3, which summarises the results of the final LSQ fits, 2450 IR transitions, made up from nearly equal numbers of P-, Q-, and R-branch lines of the v_3-band, could be fitted with a standard deviation of 2.4×10^{-4} cm^{-1}, while the 1048 IR transitions of the weak v_4-band gave the slightly larger deviation of 2.7×10^{-4} cm^{-1}. Inclusion of the purely rotational transitions within each of the two states with a weight factor of 100 (which represents the ratio by which the MW frequency measurements are estimated to be superior in precision to FT-IR peak wavenumbers) reduces these standard deviations by a factor of ~ 20. While the uncertainties in the rotational parameters of v_3 and v_4 are very comparable with their counterparts in the GS of furazan (Table 1), the values for the band origins emerge from the final fits with statistical uncertainties of less than

2×10^{-6} cm^{-1}. – As an indication of the quality of these fits both correlation matrices are reproduced above.

IV. Discussion

The successful analyses of the IR bands v_3 and v_4 confirm the initial assumption (Section II, above) that no detectable Coriolis interactions occur between these two states and other excited vibration states of furazan. On symmetry grounds alone the B_1-states $v_{11} \sim 1175$ cm^{-1} and $v_{12} \sim 953$ cm^{-1} are capable of coupling with the A_1-states $v_4 \sim 1036$ cm^{-1} and $v_3 \sim 1316$ cm^{-1} via a C-type Coriolis interaction. But v_{11} is obviously too far removed in energy (~ 140 cm^{-1}) from both v_3 and v_4 to make such effects observable. Equally, v_{12} is separated from v_4 by ~ 83 cm^{-1} and by more than four times as much from v_3, and this renders Coriolis effects again unobservably small. This finding was of course anticipated from the fact that the previously examined band v_{11} and v_{12} showed no detectable perturbations [1 c, d]. All five modes of furazan studied to date (v_{12}, v_5, v_4, v_{11}, and v_3) are therefore free from detectable interactions with each other. Hence they conform with the fundamental

assumption underlying the computer package by Gambi et al. [4].

The rovibrational assignments of peaks within the high-resolution IR-bands were helped considerably by the availability of the rotational constants of both excited states from the earlier DRM MW study [1a]. Those data fixed the structures of the IR-bands and left only the band origins as somewhat uncertain parameters. However, for an isolated and reasonably intense B-type band, such as v_3 in the present study, this uncertainty can be removed rather easily through the identification 'by inspection' of the weak, conjugate Q-branch transitions with which the absorptions on either side of the band origin begin. As a little reflection will clarify, the pattern of these (and other conjugate) transitions of an IR band will become exactly symmetrical to v^0 if the two states involved in the band (here: GS and $v_3 = 1$) have precisely the same rotational parameters. While this is probably rarely the case in reality, the variation of rotational constants between the GS and fundamental levels in furazan does not exceed 1% of the values of the GS constants and, as a consequence, there occurs a recognisable, nearly symmetrical pattern of weak absorptions for the lowest values of $J = J'$ at the start of the band on either side of the origin v^0. For A- and C-type bands this very helpful feature is hidden by the high-J Q-branch transitions which qualitatively characterise the area of the band origin in those cases. – In the weak v_4-band, where the central area is masked by transitions of the strong v_5-band, such conjugate Q-branch transitions could not be identified, and the previous DRM MW data therefore had to assume the decisive role for the assignment of this IR band: Although only six R-branch transitions within the excited state and with the lowest values of J' were available (appendix of [1a]), those transitions in conjunction with 83 Q-branch lines within v_4 provided the crucial criterion for the selection of the correct J'-values for the R-branch clusters of the FT-IR band.

The numerical results collected in Table 3 underline the conclusions drawn from the previous studies [1c, d]: The uncertainties in the rotational constants A and B of the excited states are reduced by factors of about 4 and the distortion constants, which are considered more reliably determinable than in MW spectroscopy from the large number of P- and R-branch transitions extending to high J-values in the IR bands, have their uncertainties reduced by about 2 through the inclusion in the LSQ fits of some 90 purely rotational transitions within each state. The most drastic effect of the MW data occurs in the uncertainties of the band origins. These are reduced by more than an order of magnitude from their values derived by a fit of the IR transitions alone. Although the internal consistencies which were achieved for the two band origins ($\sigma < 2 \times 10^{-6}$ cm^{-1}) cannot be exploited at present as a consequence of the significantly larger uncertainty, which is superimposed on them by the calibration of the spectrometer, the two band origins determined in the present study appear quotable with an absolute uncertainty of $\pm 10^{-4}$ cm^{-1} as $v_3^0 = 1316.2254$ cm^{-1} and $v_4^0 = 1036.1689$ cm^{-1}.

[1] O. L. Stiefvater, Z. Naturforsch. a) **45a**, 1117 (1990); b) **30a**, 1742, 1756 (1975); c) **46a**, 841 (1991); d) **47a**, 499 (1992).
[2] G. Guelachvili and K. N. Rao, Handbook of Infrared Standards, Academic Press, London 1986.
[3] J. K. G. Watson, in: Vibrational Spectra and Structure (J. R. Durig, ed.), Vol. 6, Elsevier, Amsterdam 1977.

[4] A. Gambi, M. Winnewisser, and J. J. Christiansen, J. Mol. Spectroscopy **98**, 413 (1983).
[5] D. H. Christensen, P. W. Jensen, J. T. Nielsen, and O. F. Nielsen, Spectrochim. Acta **29A**, 1393 (1973).